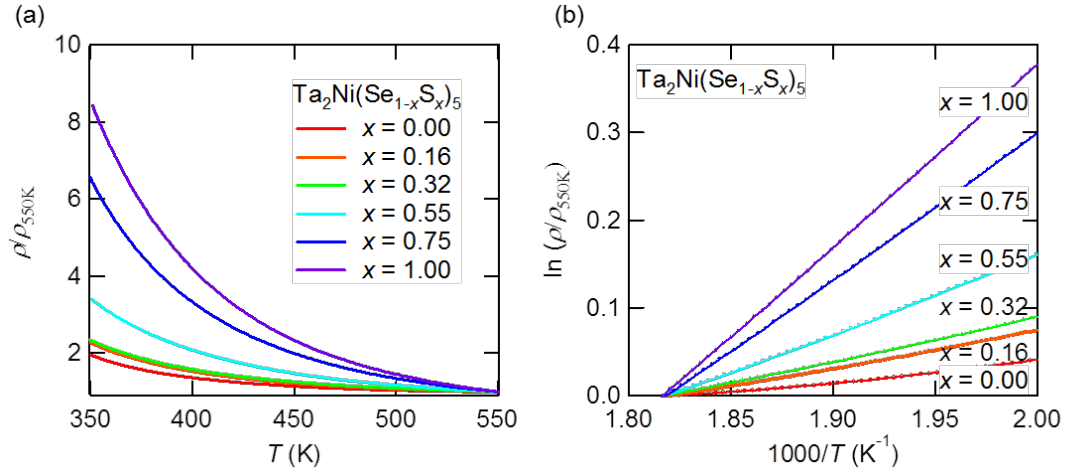
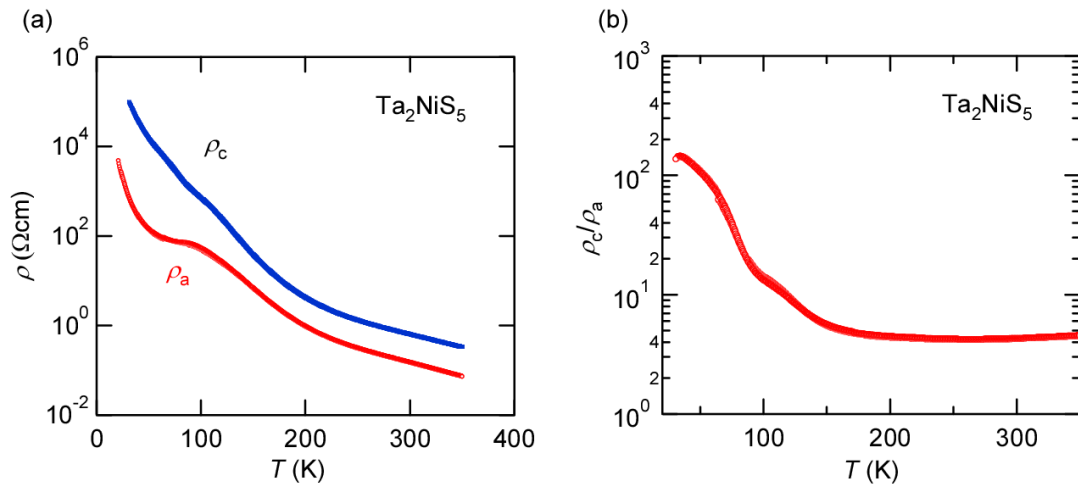


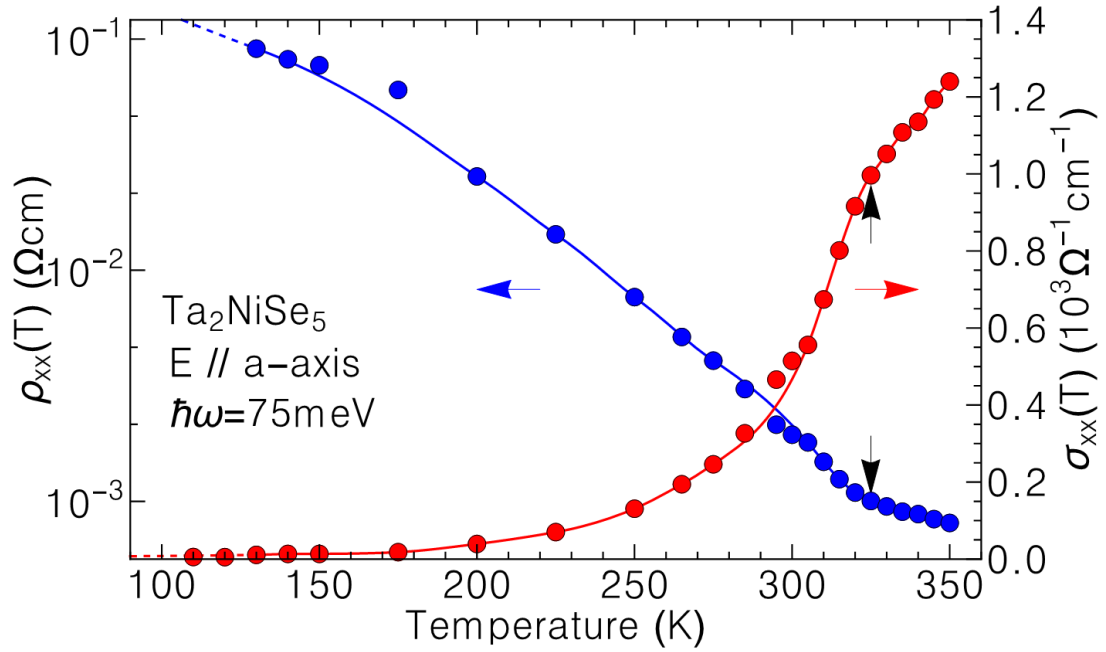
## Supplementary Figures



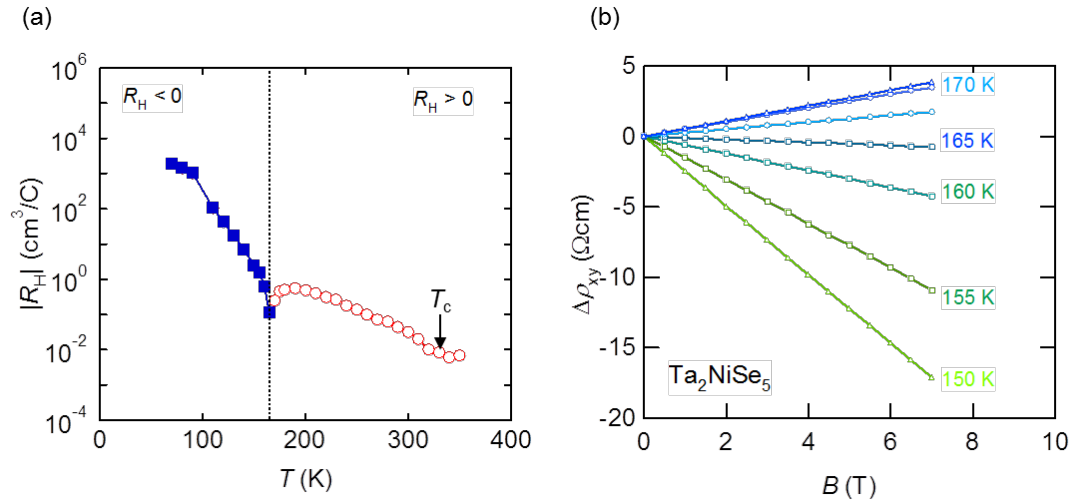
**Supplementary Figure 1 | High temperature resistivity of sulfur substituted Ta<sub>2</sub>NiSe<sub>5</sub>** (a) Electronic resistivity of sulfur doped Ta<sub>2</sub>NiSe<sub>5</sub> in the temperature range of 350 K to 550 K (normalised to 550 K). (b) Corresponding Arrhenius plot. The reported band calculations indicate that the valence band of Ta<sub>2</sub>NiSe<sub>5</sub> is composed of Ni 3d and Se 4p orbitals. With increased sulfur doping, the hybridization between Ni 3d and Se 4p (S 3p) orbitals is weakened since the energy levels of the S 3p orbitals are lower than those of the Se 4p orbitals. This eventually lowers the energy level of the valence band while the conduction band is less affected, resulting in an overall enhancement of the energy gap compared to Ta<sub>2</sub>NiSe<sub>5</sub>. Tellurium doping, on the other hand, pushes the system in the opposite direction. The stronger hybridization between Ni 3d and Te 5p orbitals leads to the valence bands being at higher energy which drives the system to be more metallic. Supplementary Fig. 1a shows high temperature resistivity ( $I \parallel a$ -axis) in the temperature range of 350 K to 550 K. The corresponding Arrhenius plot of  $\ln\rho$  is shown in panel b. In the case of a simple semiconductor with energy gap  $E_G$  the resistivity  $\rho$  as a function of temperature  $T$  in the high temperature intrinsic regime is proportional to  $\rho \propto \exp(E_G/2k_B T)$ . The experimentally defined activation energy  $E_\rho = -k_B T^2 (\partial \ln\rho / \partial T)$  at high temperatures therefore reflects  $E_G$ . It is clearly seen that the experimental activation energy is systematically enhanced (larger slope) with increased sulfur content,  $x$ .



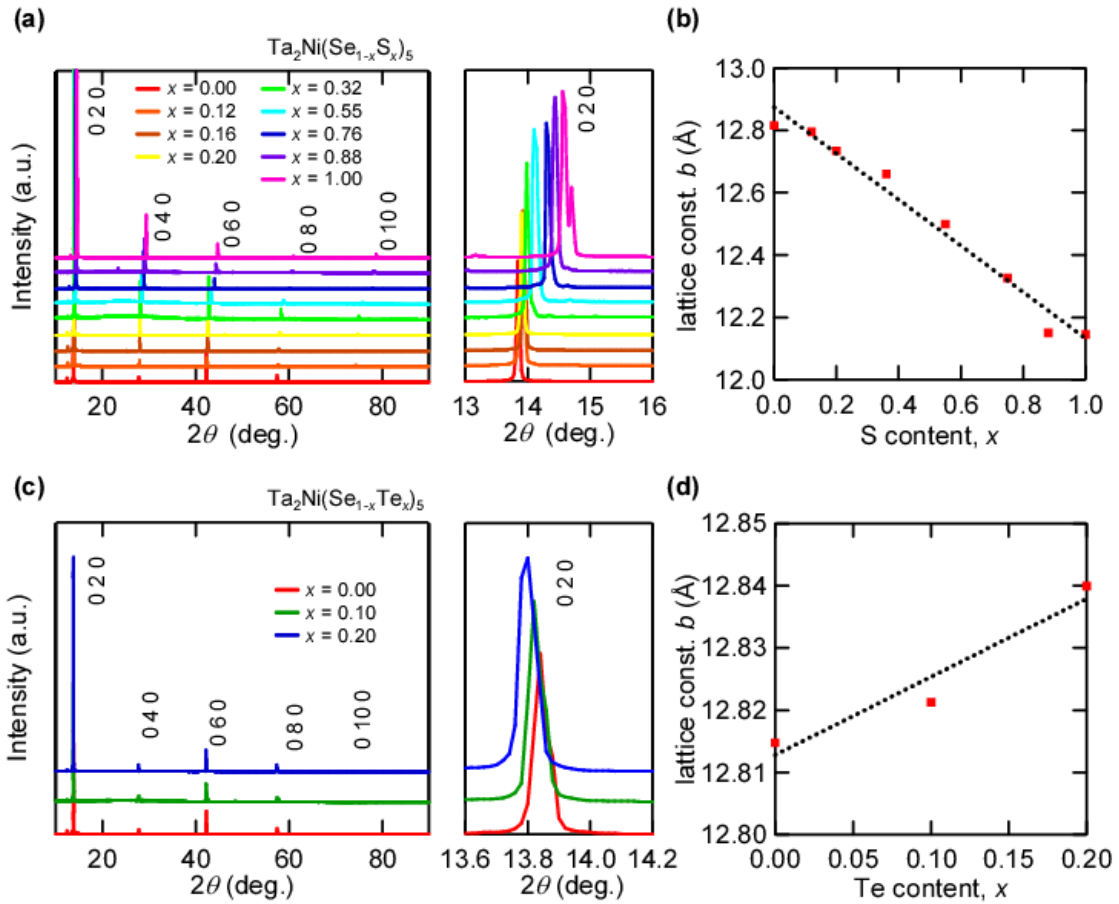
**Supplementary Figure 2 | In-plane anisotropy of Ta<sub>2</sub>NiS<sub>5</sub>** (a) The electronic resistivity of Ta<sub>2</sub>NiS<sub>5</sub>. The electric current is applied along the *a*-axis (red) and *c*-axis (blue) (b) The electronic anisotropy ratio  $\rho_c/\rho_a$ . The quasi-one-dimensionality becomes significant with lowering temperature. In contrast to Ta<sub>2</sub>NiSe<sub>5</sub>, as discussed in the main text, Ta<sub>2</sub>NiS<sub>5</sub> does not exhibit any phase transition down to 2 K. The in-plane anisotropy ratio ( $\rho_c/\rho_a$ ) is estimated to be  $\sim 5$  at 350 K, comparable to Ta<sub>2</sub>NiSe<sub>5</sub>. On cooling,  $\rho_c/\rho_a$  starts increasing and reaches  $\sim 100$  at 50 K.



**Supplementary Figure 3 | Temperature dependence of the infrared conductivity** Infrared conductivity  $\sigma_{xx}$  and corresponding resistivity  $\rho_{xx}=1/\sigma_{xx}$  of  $\text{Ta}_2\text{NiSe}_5$  vs. temperature measured at photon energy of 75 meV and electric polarization parallel to the  $a$ -axis. The filling of the electronic states within the optical gap ( $\hbar\omega = 75 \text{ meV} < E_{\text{op}} \approx 160 \text{ meV}$ ), expressed in terms of the inverse optical conductivity ( $\rho_{xx} = 1/\sigma_{xx}$ ) closely follows the behavior of the dc transport data (Fig. 2a) with a similar kink near the transition at  $T_C = 326 \text{ K}$ .



**Supplementary Figure 4 | Hall signatures of  $\text{Ta}_2\text{NiSe}_5$**  (a) The measured Hall coefficient of  $\text{Ta}_2\text{NiSe}_5$  in the temperature range of  $70 \text{ K} < T < 350 \text{ K}$  and (b) Hall signal as a function of magnetic field. The black arrow indicates  $T_c$ . The  $R_H$  value was estimated to be  $+7 \times 10^{-3} \text{ cm}^3/\text{C}$  at 350 K and found to be increasing rapidly below  $T_c$ . The  $R_H$  changes its sign at  $\sim 170 \text{ K}$ , evidencing the co-existence of electrons and holes.



**Supplementary Figure 5 | XRD analysis of pure and sulfur/tellurium-substituted  $\text{Ta}_2\text{NiSe}_5$**

(a) X-ray diffraction (XRD) pattern of sulfur- and (c) tellurium-substituted  $\text{Ta}_2\text{NiSe}_5$  single crystals taken at room temperature. The  $(0\ b\ 0)$  ( $b = 2, 4, 6, 8$  and  $10$ ) peaks are systematically shifted towards higher and lower  $2\theta$  angle, respectively. The lattice constant  $b$  of the samples is summarized in (b) and (d) respectively. Single crystalline samples were synthesized using the chemical vapour transport method. Powders of elemental tantalum, palladium and sulfur were mixed with a starting composition of 2:1:5, and loaded into an evacuated quartz tube ( $\sim 1 \times 10^{-3}$  Pa) with iodine as transport agent. The mixture was sintered under a temperature gradient of 950/850 °C. After sintering for 1 week, needle-like single crystals were grown at the cold end of the tube. The lattice constant of  $\text{Ta}_2\text{Ni}(\text{Se}_{1-x}\text{S}_x)_5$  shrinks as the sulfur content increases while tellurium substitution enlarges the lattice constant. It is concluded that chemically substituted  $\text{Ta}_2\text{NiSe}_5$  was successfully synthesized since the change of lattice constant follows Vegard's rule.